J Sol-Gel Sci Technol
DOI 10.1007/s10971-010-2193-x

ORIGINAL PAPER

Luminescent hybrid oxydiacetic/ethyleneglycol/TEOS/Eu(III) material: thermal and spectroscopic analysis

M. Claudia Marchi · Pedro F. Aramendía · Beatriz C. Barja

Received: 15 November 2009 / Accepted: 4 March 2010

Abstract A luminescent hybrid organic–inorganic material was synthesized with the sol-gel technique by hydrolysis of tetraethoxysilane (TEOS) and an organic precursor obtained through the esterification of oda (oxydiacetic acid) and EG (ethyleneglycol) in acid media. The Eu(III) ion was included in the system to monitor the formation of the complex between the lanthanide and the ligand oda in the hybrid matrix. The spectral features of the emission of the Eu(III) ion together with the data obtained from infrared spectroscopy, thermogravimetric and differential thermal analysis, and scanning electron microscopy permit the structural characterization of the system and its comparison with a reference sample in which no organic moieties were hydrolyzed during the sol–gel process.

Keywords Sol–gel · Europium(III) complexes · TEOS · Luminescence and DCCA

1 Introduction

The incorporation of lanthanide ions in hybrids matrices obtained by the sol–gel technique has been and is one of the most promising methods to fabricate optical materials [1–4]. The sol–gel method is a very useful technique to complex lanthanide ions in a solid matrix due to the mild conditions of synthesis and the relative ease of preparation and handling [5–7]. In particular, the luminescent properties of Eu(III) complexes have been extensively studied by many researchers due to their unique properties such as long excited state lifetimes (in the ms time range) and narrow emission bands [8, 9]. Non-radiative deactivation of Eu(III) is known to be highly suppressed when the coordination sites of the ion are occupied by ligands capable of preventing the direct binding of O–H (water mainly) or N–H oscillators to the metal ion [10]. This yields longer excited state lifetime and much more luminescent intensity.

In addition, Eu(III) has the special ability to monitor the environment in which it is located, a property widely used as a tool to obtain information related to the symmetry of the system under study [11–14]. It is well known that the electric dipole transition ($^5D_0 \rightarrow {}^7F_2$) originated from the $4f^6$ electronic configuration of the Eu(III) is hypersensitive which means that it is greatly affected by the coordination environment in which the ion is located. On the other hand, the magnetic dipole transition ($^5D_0 \rightarrow {}^7F_1$) is almost insensitive to the medium and can be used as an internal standard. Thus, the ratio of the intensities between the $^5D_0 \rightarrow {}^7F_2$ and the $^5D_0 \rightarrow {}^7F_1$ bands provide very useful microscopic information of the local symmetry in which the ion locates and can be used as a parameter to indicate the structure of a purely inorganic [15] or hybrid sol–gel sample and its evolution during ageing. An important advantage of using Eu(III) as a structural probe when compared with organic dyes relies on the fact that the samples can be heated up to temperatures at which all dyes would decompose or oxidize.

In this work, we compare the luminescent properties of two sol–gel silicate luminescent systems. In one of them,

M. C. Marchi · P. F. Aramendía · B. C. Barja (✉)
INQUIMAE and Departamento de Química Inorgánica, Analítica y Química Física, Facultad de Ciencias Exactas y Naturales, Universidad de Buenos Aires, Pabellón 2, Ciudad Universitaria, C1428EHA Buenos Aires, Argentina
e-mail: barja@qi.fcen.uba.ar

M. C. Marchi
e-mail: marchi@qi.fcen.uba.ar

P. F. Aramendía
e-mail: pedro@qi.fcen.uba.ar

Published online: 20 March 2010

an organic oligomer synthesized by esterification between the oxydiacetic acid (oda) and ethyleneglycol (EG) was used as a precursor for the hydrolysis of the tetraethoxysilane (TEOS) using Eu(III) ion as a probe. The detailed monitoring of the intensities of the Eu(III) bands with time along the hydrolysis-condensation process of the sample was performed and useful information of the gel structure was obtained. In the other system, the ligand oxydiacetic acid (oda) was physically entrapped inside a silicon matrix in the form of the $Na_3[Eu(oda)_3]$ complex [16]. The luminescent spectra of the Eu(III) ions in these two systems are compared and analyzed to obtain structural information of the hybrid system.

The inclusion of EG in the system has two purposes: (1) as a linker between oda and the silica matrix via the ester group and (2) as a drying control chemical additive, DCCA. These kind of additives are used to avoid the development of cracks originated from the stress generated during the evaporation process when the system goes from a wet to a dry gel. Organic additives such as polyethyleneglycol [17], formamide [18], acetamide, glycerol, oxalic acid diethyleneglycol, ethyleneglycol [19–21] or N,N-dimethylformamide [21] were incorporated into sol–gel systems to study their effects on the monolithicity, and on the optical and mechanical properties of the samples. As stated in the literature, the effect of EG on the drying process is explained mostly by the formation of strong hydrogen bonds with the Si–OH groups of the matrix [21, 22]. To this respect, we take advantage of the emission properties of the Eu(III) ion as a structural probe to get direct information of the evolution of the chemical environment that this ion monitors during the formation of the hybrid Si-EG-oda-EG-Si gel mainly as a function of time and temperature. In addition, infrared absorption, thermal analysis (TG and DTA), X-rays diffraction (XRD), and scanning electron microscopy (SEM) studies were used to characterize the samples.

2 Experimental procedure

2.1 Chemicals

Oxydiacetic acid ($HOOC–CH_2–O–CH_2–COOH$, H_2oda) and EG were obtained from Merck and ethanol from Mallinckrodt. Water was from a Milli-Q system. Tetraethoxysilane (TEOS) and tetramethoxysilane (TMOS) were obtained from Aldrich.

Lanthanide Compounds: $Na_3[Eu(oda)_3]\cdot 2NaClO_4\cdot 6H_2O$ (hereafter $Euoda_3$), was synthesized according to literature methods [14]. $Eu(NO_3)_3\cdot 6H_2O$ 99%, was obtained from Fluka Chemie AG and was used as received.

2.2 Sample preparation

2.2.1 *Hybrid ethyleneglycol-oxydiacetic acid TEOS xerogel doped with $Eu(NO_3)\cdot 6H_2O$*

Synthesis of the EG-oda ester 3.7×10^{-2} mol of EG, 4.6×10^{-3} mol of oda and 2.3×10^{-4} mol of $EuNO_3\cdot 6H_2O$ were mixed under heating while stirring until a translucent colorless solution was obtained. Final molar ratio was oda:EG:Eu = $1{:}8{:}6 \times 10^{-3}$.

Synthesis of the hybrid (EG-oda-EG) silica matrix (EuodaEG-TEOS): The final translucent solution previously obtained was added slowly to 2 mL of a 1:1 prehydrolyzed ethanolic TEOS:H_2O solution (8.9×10^{-3} mol of TEOS) at pH = 1.5 (adjusted with microliters of HCl) under stirring at room temperature. Final molar ratio was TEOS:EG:oda:H_2O:Eu = $1{:}4{:}0.5{:}4.1{:}2.5 \times 10^{-2}$. This sol was left in a sealed flask at room temperature. After a period of 26 months, measurements were performed on the transparent monolith xerogel obtained. Slices were grounded and heated at different temperature prior to spectroscopic or thermal measurements.

2.2.2 *TMOS-$Na_3[Eu(oda)_3]$ doped xerogel ($Eu(oda)_3$-TMOS)*

Sol–gel samples were prepared by hydrolysis of TMOS in acid catalyzed ethanolic medium (TMOS:EtOH:H_2O = 1:2.5:6.5 in moles) at pH = 2.5 (with HCl). 1.5 mL of anhydrous ethanol containing 35 mg (3.6×10^{-5} mol) of $Na_3[Eu(oda)_3]$ dissolved in 1.25 mL of HCl 1×10^{-3} M were added to 1.5 mL of TMOS (0.01 mol) while stirring. pH was adjusted with HCl while stirring and a transparent, colorless sol was obtained. After the sol gellified (18 h), it was left aging at room temperature in a sealed tube for 2 days. Finally it was placed in an oven at 50 °C for 14 h. After an aging period of 16 months, the dry monolith was ground manually to a fine white powder to perform the spectroscopic measurements.

2.3 Characterization techniques

All infrared spectra were recorded in KBr pellets with a Nicolet Magna 510 Fourier transform infrared (FTIR). The spectral resolution was 4 cm^{-1} for all measurements and all single beam IR spectra were the result of 32 coadded interferograms.

Powder diffraction data were obtained by a Siemens D-5000 Diffractometer with CuK_α radiation (λ = 1.542 Å) by step scanning 2θ from 3° to 40° with a step size of 0.025° and a step time of 1.2 s. The XRD peaks were deconvoluted using a multi peaks function analysis program (Origin). Three Gaussian functions were used for the

deconvolution of the hybrid matrix XRD diffractogram and a third order polynomial was used as a baseline between $2\theta = 4.5°$ and 32.0°.

Termogravimetric (TG) and Differential thermal analysis (DTA) were performed with a TGA-51 Shimadzu and DTA-50 Shimadzu instruments, respectively, from 25 to 600 °C with a heating rate of 6 °C/min in Pt crucibles under N_2 or N_2/O_2 atmosphere (flow rate 20 mL/min).

Scanning electron microscopy was carried on using a SEM Zeiss Supra 40 microscope equipped with a field emission gun (CMA, FCEN-UBA). The images were taken with in-lens detector and 5 kV acceleration voltage. The samples were placed on an aluminum holder, supported on conductive carbon tape.

Steady state emission spectra of all the compounds were recorded on a PTI QuantaMaster QM-1 luminescence spectrometer. Excitation and emission wavelengths were always 394 nm and 615 nm, respectively. Excitation and emission bandwidths were set to 2 nm and 0.5 nm, respectively.

3 Results and discussion

3.1 Microstructural characterization

3.1.1 FTIR

Figure 1 shows the FTIR spectra of the hybrid *(EuodaEG-TEOS)* gel heated in an oven for 2 h at 70, 200, 245, 295, 350 and 550 °C together with the spectrum of free oda at room temperature in the 4000 to 400 cm^{-1} range. These temperatures were chosen according to the results obtained from the evolution of the DTA curve in the presence of oxygen (as shown in Fig. 2). The band at 1734 cm^{-1} (spitted into two) in free solid oda (lowest spectrum in Fig. 1) is assigned to the stretching of the carbonyl group ($\nu_{C=O}$) [23]. It shifts to higher wavenumbers (c.a. 1748 cm^{-1} at 70 °C) in the spectra of the hybrid matrix as expected for a more localized C=O bond in an ester group (1740 ± 15 cm^{-1}) [24]. The shift is not due to the coordination of oda with Eu(III). This coordinated carboxylates make a minor contribution because oda:Eu(III) ratio is 20:1 in EuodaEG-TEOS. The sharp band at 920 cm^{-1} assigned to the γ_{OH} vibration of the carboxylic acid in the free oda disappears when the hybrid matrix is formed, providing also evidence of the esterification reaction.

The band assignment for the free EG is not straightforward if we consider that the vibration bands associated with this molecule (mainly OH stretchings at 3500 cm^{-1}, CH_2 stretchings at 2800–3000 cm^{-1} and CH_2 deformations at 1500–1300 cm^{-1}) are also found in the oda moiety or in the water molecules present in the matrix.

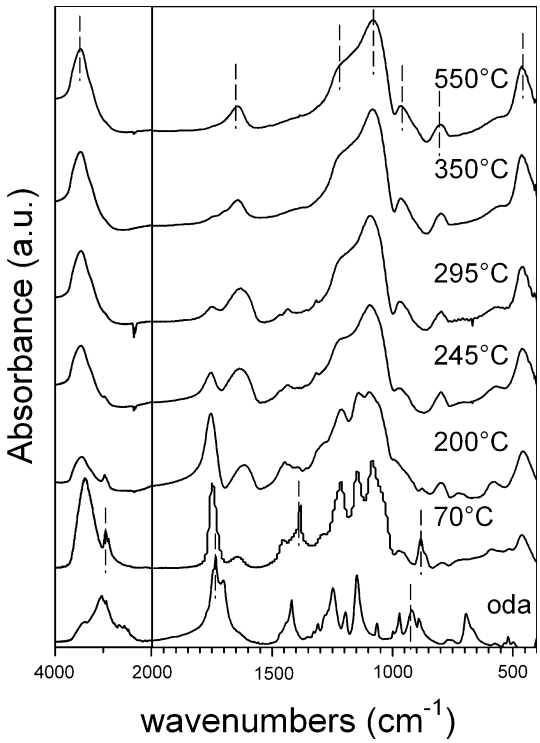

Fig. 1 FTIR spectra of the hybrid EuodaEG-TEOS gel at 70, 200, 245, 295, 350, and 550 °C together with the spectrum of free oda at room temperature. (Spectra were shifted upwards for clarity). *Vertical lines* were added to point out specific wavenumber values (See text). The 2000–400 cm^{-1} range was expanded for clarity

However, the free or bonded EG can be tracked by inspecting the evolution of the band at 883 cm^{-1} with temperature, which is characteristic of the deformation vibration of the C–C bond in EG [19]. This band can be observed in the spectra of Fig. 1 at 70 °C and to a less extent at 200 °C, but is absent at 245 °C. These results suggest that the free or hydrogen bonded EG is no more present in the hybrid matrix at temperatures higher than 200 °C. It is worth noticing that the stretching of the carbonyl group ($\nu_{C=O}$) of the ester is present in the infrared spectrum of the hybrid matrix in the 70–295 °C temperature range and disappears at 350 °C. The bands located at 2800–3000 cm^{-1}, corresponding to the CH_2 stretching vibrations of the EG and the ester, are also absent at 350 °C indicating that the organic matter was completely eliminated from the matrix at this temperature.

The broad bands in the 800–1250 cm^{-1} range correspond to the Si–O–Si, SiO–C, and Si–OH vibrations of the silica network. These bands are superimposed with those of the Si–O–C moieties arising from the hybrid silicon matrix obtained by the hydrolysis of TEOS with the ester previously formed between EG and oda. Therefore, any band assignment related with the oda moiety itself or with the EG in this wavenumber range is not straightforward.

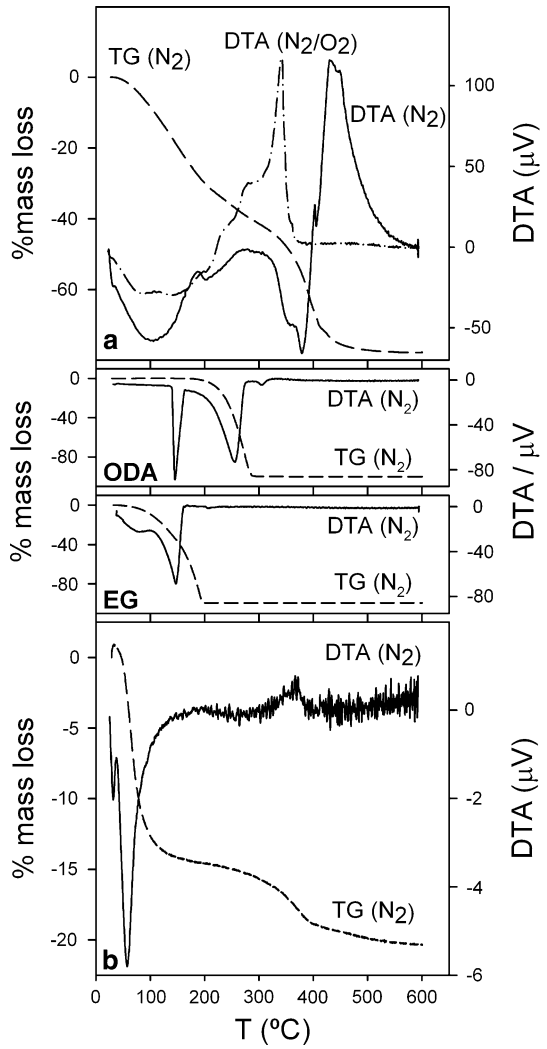

Fig. 2 **a** TG (in N_2) and DTA (in N_2/O_2 and N_2) curves for EuodaEG-TEOS **b** TG and DTA curves in N_2 for the $Eu(oda)_3$–TMOS. The TG and DTA curves in N_2 of the pure components (oda and EG) are given for comparison

The spectrum at 550 °C shows the typical profile of a silica matrix [25]. The wide band centered at 3450 cm^{-1} is attributed to the stretching of OH groups, while the one at 1643 cm^{-1} is assigned to the deformation vibrations of the H–O–H bonds indicating the presence of water in the matrix. The most intense 1084 and 1200 cm^{-1} bands are assigned to the TO and LO modes of the asymmetric Si–O stretching vibration, respectively. The bands at 800 cm^{-1} and at 965 cm^{-1} are assigned to the symmetric Si–O vibration mode and to the Si–OH stretching of terminal silanol groups, respectively. The band centered at 462 cm^{-1} can be associated with the rocking motion of the oxygen atom about an axis perpendicular to the Si–O–Si plane [26] or/and with the Si–O–Si bending mode. Its wavenumber value increases from 458 cm^{-1} (200 °C) up to 462 cm^{-1} (550 °C) along with an increase in its intensity with respect to the Si–O asymmetric stretching vibration. The fact that the band at 965 cm^{-1} does not reduce its intensity relative to the Si–O stretching is indicating that the matrix maintains a high content of terminal silanol groups, and that the condensation process above 295 °C yields a matrix with poorly crosslinked regions. This poor crosslinking is in line with the fact that the organic moieties bound to the inorganic silica network are no longer present at temperatures higher than 350 °C and therefore a decrease in the Si–O stretching frequency with temperature is observed (1093 cm^{-1} at 295 °C against 1081 cm^{-1} at 550 °C).

In *$Eu(oda)_3$-TMOS* xerogel the $Eu(oda)_3$ complex was added as a probe and can not be detected in the IR spectrum. This sample shows the typical features of a pure silica xerogel [22] (Figure not shown).

3.1.2 DTA and TG

Figure 2a and b show the DTA and TG curves for the hybrid *EuodaEG-TEOS* and the reference *$Eu(oda)_3$-TMOS* samples, respectively. The DTA of *EuodaEG-TEOS* xerogel, was performed under O_2/N_2 and N_2 atmosphere. Both DTA curves have similar features in the 25–220 °C range showing broad endothermic peaks. In addition, the TG shows a rapid weight loss (32%) which can be attributed to the evaporation of volatile products resultant from the condensation reactions as well as to the free EG present in the matrix (boiling point of EG 196 °C). The IR spectra confirm these results by inspecting the band at 883 cm^{-1} which is present with a very low intensity at 200 °C but is absent at 245 °C (Fig. 1).

The most relevant information of the thermal behavior of the sample in presence of O_2 is observed in the DTA in the 220–350 °C temperature range where a sharp exothermic peak at 340 °C with two shoulders centered at 236 and 280 °C are observed. These peaks are absent in the DTA curve measured under inert conditions and can therefore be associated with oxidative processes of the organic moieties present in the matrix. The chemical interaction of EG and polyols with the silanol groups of a silica matrix was previously reported by Stefanescu et al. [19, 27] where the EG condenses at one or both hydroxyl groups to form a hybrid matrix. The shoulder observed at 280 °C is in good agreement with the temperature reported by these authors for the elimination of EG in the silica matrix (270–290 °C). From the evolution of the stretching vibration band of the carbonyl group at 1750 cm^{-1} in the infrared spectra taken from 200 °C up to 350 °C (Fig. 1), it is clear that the oda fragments of the oda-ester bounded to the matrix are eliminated in the temperature range 300–350 °C. Following this reasoning, the strong exothermic peak centered at 340 °C can be assigned to the

oxidation of these organic groups present in the matrix. In the TGA, a slow mass loss of 15% and a rapid mass loss of 30% are observed in the 200–450 °C temperature range. These mass changes can now be assigned to the non oxidative decomposition of the organic oda-EG moieties of the hybrid matrix and are accompanied by a broad endothermic peak centered at 480 °C. The splitting observed in this peak can be possibly ascribed to the different EG-oda chains resulting from the esterification process in the initial step of the synthesis.

In the 350–600 °C temperature range, a broad exothermic peak centered at 480 °C in the DTA with no associated weight loss can be attributed to the irreversible structural relaxation process of the matrix as expected for acid-catalyzed systems with low H_2O/TEOS mole ratios [28].

Pure oda presents two endothermic peaks (Fig. 2) when its DTA analysis is performed under inert conditions. At 146 °C, a sharp endothermic peak is observed evidencing the melting point of the acid while a second and broader endothermic peak at 254 °C arises from the evaporation of the anhydride of the acid, formed during the heating of the sample [29]. The TG curve shows a single weight loss of 100% in the 200–280 °C temperature range. From DTA curve for pure EG (Fig. 2), measured under N_2 atmosphere a sharp endothermic peak at 146 °C with a broad shoulder centered at 78 °C is observed. At same experimental conditions its TG presents a single 100% weight loss between 60 and 200 °C at which EG is totally eliminated.

According to these results, the temperature values at which oda and EG moieties are oxidized (in air) or decomposed (under N_2) in the hybrid matrix are above the temperature values at which these two reactants are eliminated when they are pure evidencing true chemical interactions with in the matrix.

The *Eu(oda)$_3$-TMOS* matrix can be considered a reference sample in which neither EG nor oda acid were added to form an hybrid matrix. The elimination of the oda from the Eu(oda)$_3$ complex can not be observed in the TG analysis (Fig. 2b) due to its low concentration (TMOS: oda = 280:1). The TG curve for this matrix shows the typical features of a pure silica matrix. A 14% mass loss due to the elimination of volatile products (water, ethanol) obtained from the condensation reaction was observed in the 25–100 °C temperature range. This mass loss is observed in the DTA as a sharp endothermic peak centered at 60 °C. In a second stage, as the condensation reactions proceed, a mass loss of 4% is observed between 300 and 400 °C which can be associated with the non oxidative decomposition of the residual ethoxy groups present in the matrix as expected for a sample in which the H_2O:TMOS mole ratio is 6.5 [18, 19]. This weight loss in the TG curve is accompanied by a very weak exothermic peak (see scale) centered at 366 °C.

3.1.3 XRD and SEM

The powder XRD patterns for the hybrid *EuodaEG-TEOS* matrix and for the reference *Eu(oda)$_3$-TMOS* matrix (see Fig. 3) are very similar. While both samples are amorphous and show two broad bands at similar 2θ values, the hybrid matrix has an additional shoulder centered at $2\theta < 10°$.

From the deconvolution of the diffractogram of the *EuodaEG-TEOS* sample, three peaks were obtained at $2\theta_1 = (8.237 \pm 0.032)°$, $2\theta_2 = (12.454 \pm 0.026)°$, and $2\theta_3 = (23.303 \pm 0.029)°$ with areas of 19%; 62%; and 19%, respectively. These results are indicating the presence of a new and larger interplanar distance between silicon atoms in the hybrid *EuodaEG-TEOS* matrix which should be associated with the spacing between silicon atoms bound to the organic precursor EG-oda. From the powder X-ray patterns of ormosils of TMOS-MTMOS (methyltrimethoxysilane), a value of $2\theta_1 = 7$–$10°$ was also reported which was associated with the spacing between silicon atoms attached to the organic methyl groups. The diffraction band at the larger angle $2\theta_2 \approx 23°$ can be associated with the shorter structural distance similar to those obtained for fused silica ($2\theta = 21.16°$) and for silica xerogels obtained from 100% TMOS ($2\theta = 22.9°$) [30].

The same hybrid *EuodaEG-TEOS* samples analysed by FTIR were investigated by scanning electron microscopy to study the effects of thermal process on silica morphology. SEM micrographs in Fig. 4 reveal differences in the microstructures of the as-synthesized xerogels when the temperature was increased. An open structure can be observed for the samples of *EuodaEG-TEOS* at lower temperatures which could be indicating the poor crosslinking revealed by the FTIR spectra. The results show that the drying process diminishes the average size pore from 15.0, 11.6, 9.8, 8.3 to 6.0 nm for 200, 245, 295, 350 and 550 °C oven temperatures, respectively (shown in Fig. 4a–e). Whereas the system exhibits a homogeneous porous distribution below 350 °C, aggregates

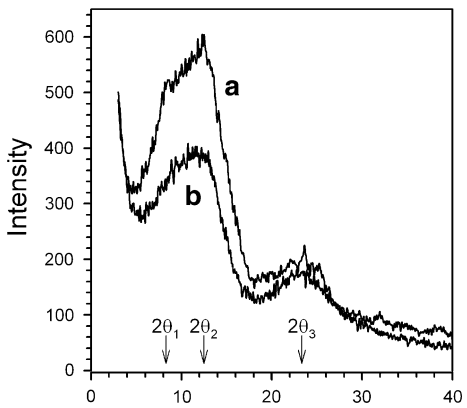

Fig. 3 X rays diffractograms for **a** Euoda-EG-oda and **b** Eu(oda)$_3$-TMOS

can be observed at 550 °C in the silica matrix. The changes in the microstructures of the samples with increasing temperature must certainly be attributed to the elimination of the EG-oda organic chains of the hybrid xerogel in agreement with the FTIR results.

Figure 4f shows the SEM micrograph of the reference sample. A stiffer network with smaller pore sizes is observed even when the sample received no thermal treatment.

3.2 Optical characterization

Figure 5 shows the evolution of the normalized emission spectra of a transparent hybrid *EuodaEG-TEOS* sample from the liquid sol (Fig. 5a) to the gel at room temperature (Fig. 5 b–e). The spectra show the characteristic Eu(III) centered emission bands ($^5D_0 \rightarrow {}^7F_J$) for $J = 0$, 1, 2, 3, and 4 at ca. 578, 590, 615, 650, and 698 nm, respectively.

The change in the intensities and splitting of the Eu(III) bands reveal the sensitivity of the Eu(III) ion to the different environments and its use as a structural probe. One

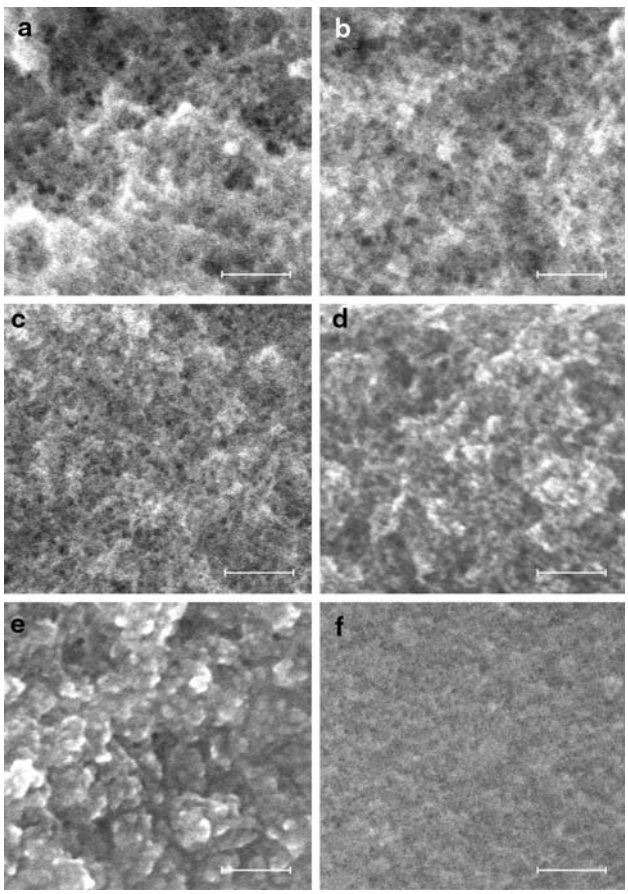

Fig. 4 SEM photographs of EuodaEG-TEOS xerogel treated thermically for 2 h at 200 °C (**a**), 245 °C (**b**), 295 °C (**c**), 350 °C (**d**), 550 °C (**e**) and Eu(oda)$_3$TMOS reference xerogel keeped at room temperature (**f**). The *bar* corresponds to 100 nm

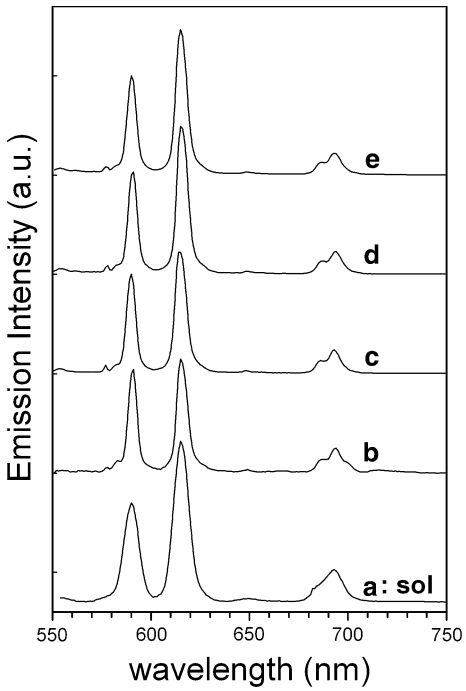

Fig. 5 Normalised emission spectra of EuodaEG-TEOS from the liquid sol (Fig. 5a) to the gel at room temperature (Fig. 5 b–e) at different aging time (for times see Fig. 6). The spectra show the characteristic Eu(III) centered emission bands ($^5D_0 \rightarrow {}^7F_J$) for $J = 0$, 1, 2, 3, and 4 at ca. 578, 590, 615, 650, and 698 nm, respectively

of the most significant features of the Eu(III) emission spectra is the amplitude of the $^5D_0 \rightarrow {}^7F_0$ (ca. 578 nm) band and its splitting. Given that both levels have $J'' = J' = 0$, no degeneracy is possible and any splitting of this band is an evidence Eu(III) occupying sites of different symmetry. Another important feature to consider in the analysis of the emission spectra of Eu(III) is the ratio of the intensities for the hypersensitive electric dipole transition ($^5D_0 \rightarrow {}^7F_2$) to the magnetic dipole transition ($^5D_0 \rightarrow {}^7F_1$), hereafter called $R = I_{F2}/I_{F1}$. The higher this ratio, the lower the symmetry of the local environment of the Eu(III) ions in the matrix [12, 31, 32] with the lanthanide occupying sites with no inversion center symmetry.

A brief analysis of the evolution of the $R = I_{F2}/I_{F1}$ ratio with time shows that in the sol, when the amount of added EG is in excess with respect to the rest of the reactants (Fig. 5a), an R value of 1.6 is measured which is very close to the one corresponding to a mixture of Eu(III) salt in pure EG ($R_{EG} = 1.8$, not shown). The spectrum in Fig. 5a is a solution-like spectrum in which the $^5D_0 \rightarrow {}^7F_0$ is absent and the bands are broader than those corresponding to the subsequent gel stages. As the hydrolysis/condensation reactions take place, the R value decreases, until it achieves a minimum value when the wet gel is formed ($R = 1.1$, Fig. 5b) to finally increase steadily with the aging process ($R = 1.2$, $R = 1.42$ and $R = 1.64$ in Fig. 5c–e,

respectively). The initial decrease in this parameter from the sol to the gel stage is an evidence of an increase in the symmetry of the system. The Eu(III) probe senses a more symmetrical environment in the first stages of the formation of the hybrid *EuodaEG-TEOS* system. This behavior can be explained considering that during the earlier stages of the sol–gel process where the viscosity of the system is lower, the carbonyls groups of the long hybrid silanol chains have more chance to get closer to the probe to coordinate the Eu(III) sites, given the high affinity of the lanthanide for the oda group. In fact, an $R = 1.1$ is quite similar to the $R = 0.95$ value obtained for the reference system *Eu(oda)$_3$-TMOS* xerogel.

It is worth noting that the time necessary to obtain a densified gel for this hybrid material was much longer than that for the reference sample. *Eu(oda)$_3$-TMOS* gelified in 18 h, and no detailed tracking of the evolution of this system with time was performed.

Figure 6 shows how the $R = I_{F2}/I_{F1}$ value increases very slowly with time and how the probe is capable of monitoring the minor microscopic changes that take place in the structure of the sample even in a very long time scale without decomposing. When the densification process is speed up by heating the gel at 60 °C for 7 h (See Fig. 7), a dramatic increase for the $R = I_{F2}/I_{F1}$ value is observed evidencing the poorly symmetric Eu(III) environment and thus suggesting that most of the carbonyl groups of the long hybrid silanol chains are no longer able to coordinate the probe. The higher splitting of the $^5D_0 \rightarrow {}^7F_0$ with increasing temperature (see Insets in Fig. 7) indicate that the probe locates at least two (60 °C) or three (600 °C) different sites. At 600 °C, where no organic moieties remain present in the *EuodaEG-TEOS* sample, as observed from the IR spectra and the thermal analysis, the R attains a value of 3 (Fig. 7). This value is similar to those obtained

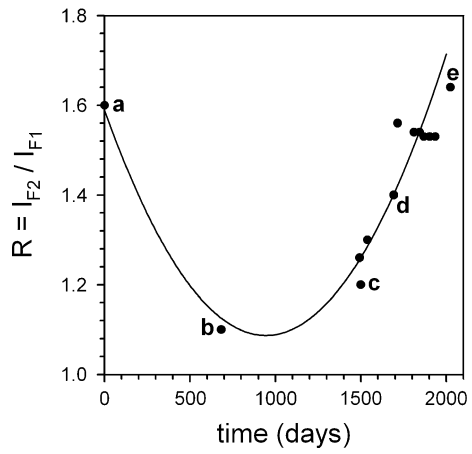

Fig. 6 Evolution of the $R = I_{F2}/I_{F1}$ ratio with time for EuodaEG-TEOS. The *letters a–e* indicate the time at which the corresponding spectra of Fig. 5 were taken

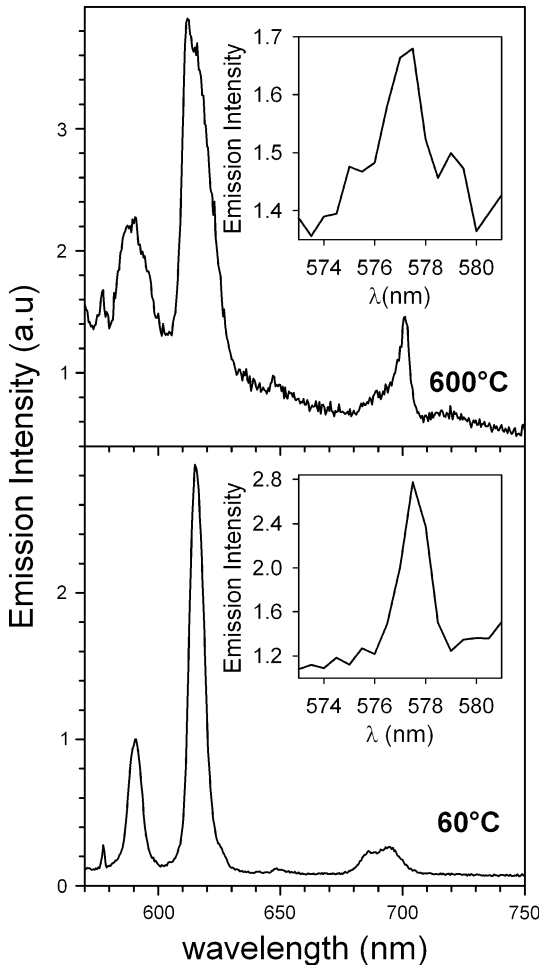

Fig. 7 Emission spectra of EuodaEG-TEOS at 60 °C and 600 °C. The insets show the $^5D_0 \rightarrow {}^7F_0$ emission band in detail at both temperatures

from the emission spectrum of inorganic silica xerogel obtained by an acid catalysed sol–gel method in which pure $Eu(NO_3)_3$ was added as a probe in a 1:4:4 TMOS: EtOH:H_2O system. R values higher than 5 were observed in Eu-chloride silica glass systems at 500 °C [11]. The bands of the emission spectrum are much broader and the J-splitting is clearly observed. In addition, the relative intensity and splitting of the non-degenerate $^5D_0 \rightarrow {}^7F_0$ band is higher while its broadening becomes larger evidencing the wide range of low symmetry sites symmetries in agreement with an amorphous glassy environment where C_s or even lower point-group symmetry were reported [9].

It is interesting to compare and analyze the emission spectrum of the hybrid sample with that of the reference sample. In Fig. 8b the emission spectra of the *Eu(oda)$_3$-TMOS* xerogel is shown ($R = 0.95$). In this sample, the Eu(III) is coordinated to three oda ligands and the complex is entrapped in the silica matrix. The emission spectrum of *Eu(oda)$_3$-TMOS* xerogel does not show the $^5D_0 \rightarrow {}^7F_0$

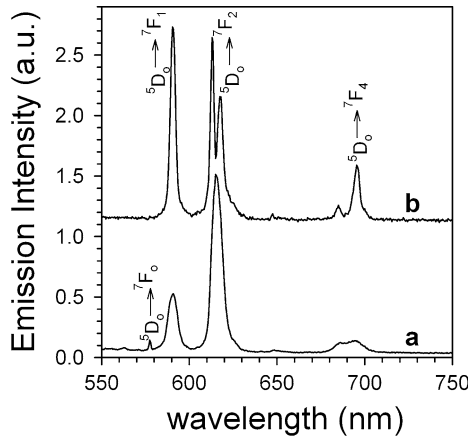

Fig. 8 Emission spectra of **a** EuodaEG-TEOS matrix after being heated at 60 °C for 7 h, $R = I_{F2}/I_{F1} = 3$ and **b** $Eu(oda)_3$-TMOS xerogel, $R = I_{F2}/I_{F1} = 0.95$

band at 578 nm when compared with the hybrid sample in Fig. 8a indicating that the sites symmetries of the Eu(III) ions in both samples are certainly different.

At this point, it is worth mentioning that the $J'' = J' = 0$ transition of Eu(III) is also absent in the emission spectrum of crystalline $Na_3[Eu(oda)_3]$ complex (not shown) as expected for the highly symmetric D_3 site occupied by the lanthanide in this complex [33]. This result shows that the ligand field sensed by the lanthanide keeps unaltered when including the crystalline complex in the silica network which is a strong evidence to conclude that the three molecules of oda coordinate the Eu(III) ion. The marked splitting of the $^5D_0 \rightarrow {}^7F_2$ band at ca. 615 nm into 2 bands is also consistent with a D_3 symmetry, in which a maximum of three peaks are expected, and might be observed if higher resolution measurements were performed.

4 Conclusions

The results of the thermal and spectroscopic measurements allow to conclude that the Eu(III) ion coordinates to the organic moieties of the hybrid matrix in the very first stages of the sol–gel synthesis where the presence of the lanthanide ion can act as a directing agent and thus coordinating the carbonyl of the oda moieties. The evolution of the spectroscopic parameter $R = I_{F2}/I_{F1}$ in real time shows that minor changes, consequence of the condensation process of the matrix, take place slowly after the gel is formed. The long organic chains collapse and fail to keep the symmetric environment in the system when the condensation and aging processes take place. At much higher temperatures R reaches the values expected for an inorganic silica matrix. The comparison of the intensity, splitting and bandwidth of the Eu(III) bands in the *EuodaEG-TEOS* hybrid sample with the reference sample *Eu(oda)$_3$-TMOS* was performed and the results show that while Eu(III) locates in sites with higher coordination symmetries (close to D_3) in the reference sample, a collection of sites with much lower symmetry point group are occupied by the lanthanide in the hybrid sample.

The sensitive Eu(III) emission allows long term montoring of gel aging and might have consequences for optical applications of Eu(III) containing glasses.

Acknowledgments BCB and PFA are members of Carrera del Investigador Científico (Research Staff) from CONICET (National Research Council of Argentina). MCM is researcher at the Universidad de Buenos Aires. The work was supported by grants UBACyTX006 (Universidad de Buenos Aires) and PICT33973 (ANPCyT, Argentina).

References

1. Carlos LD, Ferreira RAS, de Zea Bermudez V, Ribeiro SJL (2009) Lanthanide-containing light-emitting organic–inorganic hybrids: a bet on the future. Adv Mater 21:509–534
2. Binnemans K (2009) Lanthanide-based luminescent hybrid materials. Chem Rev 109:4283–4374
3. Reisfeld R, Saraidarov T, Gaft M, Pietraszkie M (2007) Luminescence of cryptate-type Eu^{3+} complexes incorporated in inorganic and ormocer sol–gel matrices. Opt Mater 29:521–527
4. Benson E, Medí A, Reyé C, Corriú RJP (2006) Functionalisation of the framework of mesoporous organisilicas by rare-earth complexes. Mater Chem 16:246–248
5. Battisha IK, El Beyally A, Abd El Mongy S, Nahra AM (2007) Development of the FTIR properties of nano-structure silica gel doped with different rare earth elements, prepared by sol-gel route. J Sol-Gel Sci Technol 41:129–137
6. Avila LR, Nassor EC, Pereira PFS, Cestari A, Ciuffi KJ, Calefi PS, Nassar EJ (2008) Preparation and properties of europium-doped phosphosilicate glasses obtained by the sol–gel method. J Non-Cryst Solids 354:4806–4810
7. Nassar EJ, Ciuffi KJ, Lima Ribeiro SJ, Messaddeq Y (2003) Europium incorporated in silica matrix obtained by sol-gel: luminescent materials. Mater Res 6(4):557–562
8. Ofelt GS (1963) Structure of the f^6 configuration with application to rare earth ions. J Chem Phys 38:2171–2180
9. Parker D, Williams G (1996) Getting excited about lanthanide complexation chemistry. J Chem Soc Dalton Trans 18:3613–3628
10. Beeby A, Clarkson IM, Dickins RS, Faulkner S, Parker D, Royle L, de Souza AS, Gareth Williams JA, Woods MJ (1999) Non-radiative deactivation of the excited ststes of europium, terbium and ytterbium complexes by proximate energy-matched OH, NH and CH oscillators: an improved luminescence method for establishing solution hydration states. J Chem Soc Perkin Trans 2:493–503
11. Reisfeld R, Zigansky E, Gaft M (2004) Europium probe for estimation of site symmetry in glass films, glasses and crystals. Mol Phy 102:1319–1330
12. Carlos LD, Sá Ferreira RA, Gonçalves MC, De Zea Bermudez V (2004) Local coordination of Eu(III) in organic-inorganic amine functionalized hybrids. J Alloys Comp 374:50–55
13. Oomen EWJL, van Dongen AMA (1989) Europium (III) in oxide glasses. Dependence of the emission spectrum upon composition. J Non-Cryst Solids 111:205–213

14. Richardson FS (1982) Terbium (III) and europium (III) Ions as luminescent probes and stains for biomolecular systems. Chem Rev 82:541–552
15. Zhang Y, Wang M (1999) The structure information given by R curve of Eu^{3+} probe during the heat treatment process of SiO_2–B_2O_3 gel glasses. Mater Lett 41:149–152
16. Albin M, Whittle RR, Horrocks WD Jr (1985) Laser spectroscopic and X-ray structural investigation of europium(III)-oxydiacetate complexes in solution and in the solid state. Inorg Chem 24:4591–4594
17. Ribeiro SJL, Dahmouche K, Ribeiro CA, Santilli CV, Pulcinelli SH (1998) Study of hybrid silica-polyethyleneglycol xerogels by Eu^{3+} luminescence spectroscopy. J Sol-Gel Sci Technol 13:427–432
18. Lenza RFS, Vasconcelos WL (2001) Preparation of silica by sol-gel method using formamide. Mater Res 4:189–194
19. Parvathy Rao A, Venkasteswara Rao A (2003) Studies on the effect of organic additives on the monolithicity and optical properties of the rhodamine 6G doped silica xerogels. Mater Lett 57:3741–3747
20. Uchida N, Ishiyama N, Kato Z, Uematsu K (1994) Chemical Effects of DCCA to the sol-gel reaction process. J Mater Sci 29:5188–5192
21. Parashar VK, Raman V, Bahl OP (1996) The role of N, N, dimethylformamide and glycol in the preparation and properties of sol-gel derived silica. J Mater Sci Lett 15:1403–1407
22. Stefanescu M, Soia M, Stefanescu O (2007) Thermal and FTIR study of the hybrid ethylene-glycol-silica matrix. J Sol-Gel Sci Technol 41:71–78
23. Ramsis H, Perez-Ruiz E, Roger J, Bourret E, Delarbre JL, Maury L (1995) Vibrational study of diglycolic acid and potassium diglycolate salts. J Raman Spectrosc 26:131–136
24. Roeges NPG (1994) A guide to the complete interpretation of infrared spectra of organic structures. Wiley, New York Chapter 7, page 174
25. Brinker CJ, Scherer GW (1990) Sol-gel science. The physics and chemistry of sol-gel processing. Academic Press, New York Chapter 9, Section 2.4.2
26. Karakassides MA, Petridis D, Gournis D (1997) Infrared reflectance study of thermally treated Li- and Cs-montmorillonites. Clays Clay Mineral 45(5):649–658
27. Stefanescu M, Stoia M, Stefanescu O, Popa A, Simon M, Ionescu C (2007) The interaction between TEOS and some polyols. Thermal analysis and FTIR. J Therm Anal Cal 88:19–26
28. Brinker CJ, Scherer GW (1990) Sol-gel science. The physics and chemistry of sol-gel processing. Academic Press, New York Chapter 9, Section 2.2.3
29. Vinciguerra V, Bucci R, Marini F, Napoli A (2006) Thermal behaviour of iminoacetic, oxydiacetic and thiodiacetic acids. J Therm Anal Cal 83(2):475–478
30. Lana SLB, Seddon AB (1998) X-ray diffraction studies of sol-gel derived ORMOSILS based on combination of tetramethoxysilane and trimethoxysilane. J Sol-Gel Sci Technol 13:461–466
31. Lavin V, Baube P, Jayasankar CK, Martín IR, Rodriguez VD (2001) On the local structure of Eu^{3+} ions in oxyfluoride glasses. Comparison with fluoride and oxide glasses. J Chem Phys 115:10935–10944
32. McDonagh C, Ennis G, Marron P, O'Kelly B, Tang ZR, McGilp JF (1992) Characterization of sol-gel glasses using optical probes. J Non-Cryst Solids 147–148:97–101
33. Kirby AF, Richardson FS (1983) Optical excitation and emission spectra of Eu^{3+} in microcrystalline samples of trigonal $Na[Eu(ODA)_3].2NaClO_4.6H_2O$. J Phys Chem 87:2557–2563